CFD ANALYSIS OF TURBULENT JET BEHAVIOR INDUCED BY A STEAM JET DISCHARGED THROUGH A VERTICAL UPWARD SINGLE HOLE IN A SUBCOOLED WATER POOL

HYUNG SEOK KANG and CHUL-HWA SONG*
Korea Atomic Energy Research Institute
Daedeok-daero 1045, Yuseong, Daejeon, 305-353, Republic of Korea
*Corresponding author. E-mail : chsong@kaeri.re.kr

Received August 06, 2010

Thermal mixing by steam jets in a pool is dominantly influenced by a turbulent water jet generated by the condensing steam jets, and the proper prediction of this turbulent jet behavior is critical for the pool mixing analysis. A turbulent jet flow induced by a steam jet discharged through a vertical upward single hole into a subcooled water pool was subjected to computational fluid dynamics (CFD) analysis. Based on the small-scale test data derived under a horizontal steam discharging condition, this analysis was performed to validate a CFD method of analysis previously developed for condensing jet-induced pool mixing phenomena. In previous validation work, the CFD results and the test data for a limited range of radial and axial directions were compared in terms of profiles of the turbulent jet velocity and temperature. Furthermore, the behavior of the turbulent jet induced by the steam jet through a horizontal single hole in a subcooled water pool failed to show the exact axisymmetric flow pattern with regards to an overall pool mixing, whereas the CFD analysis was done with an axisymmetric grid model. Therefore, another new small-scale test was conducted under a vertical upward steam discharging condition. The purpose of this test was to generate the velocity and temperature profiles of the turbulent jet by expanding the measurement ranges from the jet center to a location at about 5% of U_m and 10 cm to 30 cm from the exit of the discharge nozzle. The results of the new CFD analysis show that the recommended CFD model of the high turbulent intensity of 40% for the turbulent jet and the fine mesh grid model can accurately predict the test results within an error rate of about 10%. In this work, the turbulent jet model, which is used to simply predict the temperature and velocity profiles along the axial and radial directions by means of the empirical correlations and Tollmien's theory was improved on the basis of the new test data. The results validate the CFD model of analysis. Furthermore, the turbulent jet model developed in this study can be used to analyze pool thermal mixing when an ellipsoidal steam jet is discharged under a high steam mass flux in a subcooled water pool.

KEYWORDS : Steam Jet, Turbulent Jet, CFD, Pool Thermal Mixing

1. INTRODUCTION

The OECD Nuclear Energy Agency's Committee on the Safety of Nuclear Installations (CSNI) and its Working Group on the Analysis Management of Accidents (WGAMA) have been dealing with general reactor issues, containment thermal-hydraulics as well as new issues such as the application of computational fluid dynamics (CFD) to nuclear reactor safety (NRS) problems. Following the initiatives of the CSNI and the International Atomic Energy Agency, international experts have recently been focusing on the application of CFD to NRS problems [1]. They have analyzed the status of CFD technologies developed in technical fields other than the nuclear thermal-hydraulic field. They have also drawn up the best practice guidelines (BPG) for dealing with NRS problems [2,3], the assessment of CFD application to a single-phase flow [3], and the extension of CFD to a two-phase flow relevant to NRS problems [6]. These activities have led to the identification of some important issues and the future directions pertaining to the application of CFD tools to NRS problems.

Six NRS topics were considered for the CFD code application to two-phase flow problems. All the topics are high priority issues (as indicated by ongoing investigations); they all have a chance of being successful (maturity of present tools to handle the issue); they all have available data (of a CFD grade); they apply to all water reactors and all flow regimes; and they do not overlap with other activities of the WGAMA [4]. The six topics are dry-out, DNB, pressurised thermal shock, pool heat exchanger, steam discharge in a pool, and fire analysis. They selected a limited list of benchmarks for each NRS topics and evaluate the present capabilities and limitations with a

view of promoting the progress of CFD tools.

On the topic of steam discharge in a pool, a CFD method of analysis was developed to calculate the local pool temperature distribution for a steam jet is discharged in a subcooled water pool. This method was used for a safety analysis of an in-containment refueling water storage tank (IRWST) of the Advanced Power Reactor 1400 MWe [5-8]. The CFD analysis was also used to assist the development of empirical correlations for a simple prediction of the velocity and temperature of a turbulent water jet induced by the steam jet condensation process [8]. The developed correlations may be effectively used to evaluate the thermal-hydraulic load on the IRWST wall.

The validation stage of CFD analysis with small-scale

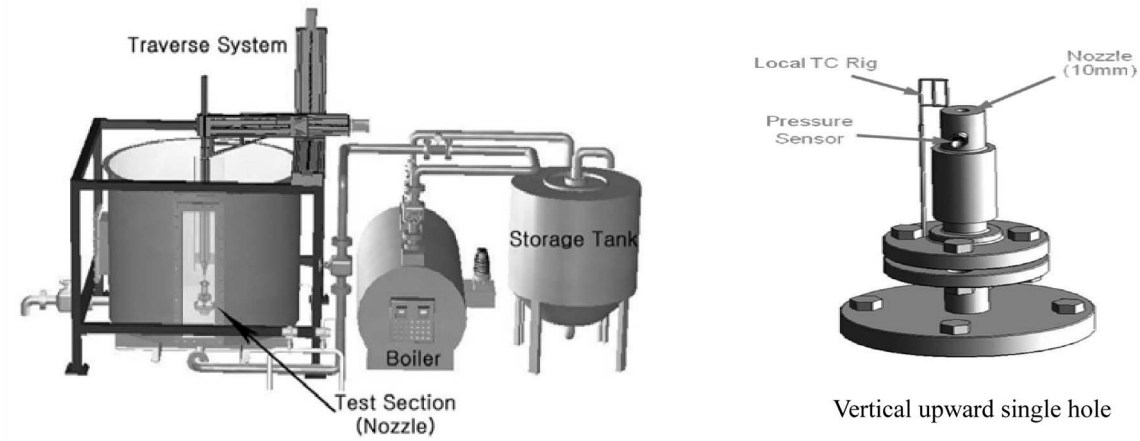

Fig. 1. The GIRLS Facility [12]

Table 1. Experimental Conditions [12]

Steam mass flux (kg/m^2s)	Pool temperature (ºC)	Axial distance along the nozzle exit (cm)	Radial distance from the jet center (cm)
450, 600, 750, 900	30, 45, 50, 55, 60, 65, 70, 75, 80, 85	10	0 – 4.05
		15	0 – 5.50
		20	0 – 8.20
		25	0 – 8.20
		30	0 – 10.3

Table 2. Measuring Devices and Uncertainty [12]

Measuring parameter	Measuring device	Uncertainty
Temperature of pool wall side (6 EAs), local (10 EAs) and turbulent jet (1 EA)	K-type TC	0.6 ºC
Steam pressure at the vertical upward hole	Rosemount 3051P	0.5 kPa
Mass flow rate of the steam jet	Rosemount 8800A	1.35 %
Velocity of the turbulent jet	Pitot tube	±2 %
Resolution of the local position	3-D Traverse System	0.01 mm

test data shows that a high turbulent intensity value (of 30% to 40%) of the mean velocity of the turbulent jet may be developed during the steam jet condensation process [8]. This high turbulent intensity may widen the turbulent jet boundary, and then the diffusion process may also increase the momentum and heat transfer along the radial direction of the turbulent jet [8,9]. This process can quickly increase the local velocity and temperature around the jet width boundary which in turn may affect the local temperature of the subcooled water at the outer region of the jet that flows into the steam jet. The final goal of the safety evaluation of the IRWST pool is to define the location and temperature of the local hot spot. The hot spot exists around the steam jet because the water heated by the thermal mixing that flows into the steam jet may yield an unstable steam condensation [10]. Therefore, it is necessary to quantify the effect of the turbulent intensity on the velocity and temperature distribution in the turbulent jet induced by condensing jets.

In a previous test, we could only measure the velocity and temperature profiles of a turbulent jet between the jet center and the jet width boundary along the radial direction and at a distance of about 8 cm to 16 cm from the exit of the steam discharge nozzle along the axial direction [11]. Moreover, the turbulent jet behavior and thermal mixing phenomenon of that test failed to show an exact axisymmetric flow pattern because the steam jet through the horizontally single nozzle was discharged in only one direction in the subcooled water pool. We therefore performed another small-scale test to obtain precise velocity and temperature data of the turbulent jet from the jet center to the end of jet width boundary and at a distance of 10 cm to 30 cm from the exit of the steam discharge nozzle. This test involved the discharge of a steam jet through a vertical upward single hole into the subcooled water pool [12].

2. SMALL-SCALE VALIDATION TEST

2.1 Experimental Facility and Matrix

A series of the steam jet discharges through a vertical upward single hole into a subcooled water pool was performed in a steam mass flux ranges of 450 kg/m^{2}s to 900 kg/m^{2}s. Fig. 1 shows vertical upward single hole; it also shows a quasi-steady state of a general investigation rig for liquid/Steam (GIRLS) jet direct condensation facility with a pool temperature in the range of 30ºC to 85ºC (Table 1) [12]. The diameter of the vertical upward single hole is 10 mm. The subcooled water tank has a diameter of 1.8 m and a height of 1.5m. The height of the free surface in the tank is maintained at 1.3m by means of a drain device. All the cases of the steam mass flux and pool temperature in the test belong to the stable condensation region of the condensation region map [13]. A 3-D traverse system with a movable pitot tube and thermocouple (TC) spool was continually moved to measure the velocity and temperature data along the axial and radial directions (Table 1). The temperature of the pool water was calculated by averaging the results of six TCs near the water pool wall. The uncertainty values of each measuring device are shown in Table 2.

2.2 Experimental Results and the Modeling of the Turbulent Jet

In this study, the experimental results of the steam jet mass flux of 900 kg/m^{2}s and the pool temperature of 30ºC, 45ºC and 60ºC (Fig. 2) are compared with the CFD results of the previously developed turbulent jet model; the conditions for the test data include a steam mass flux of 1000 kg/m^{2}s and a pool temperature of 15ºC to 47ºC under a horizontal steam discharging condition [8]. Fig. 2 shows the characteristic length of the turbulent jet width (y_c), the maximum velocity (U_m), and temperature (T_m) along the jet centerline, as well as the velocity and temperature profiles along the radial direction. As indicated in Fig. 2(a), the definition of y_c is the length along the radial direction from the centerline to a location that represents 50% of U_m. The theory of Tollmien's axisymmetric source [14] is mainly applied to a submerged turbulent flow that resembles a turbulent flow induced by the steam jet condensation in a subcooled water pool. This theory assumes that the turbulent jet flow starts from the point source and that some of the axial flow moves upward due to the turbulent shear stress while the turbulent jet propagates axially. The similarity method (Table 3) which was introduced to solve Tollmien's model depends on the coefficient of *a* which is related to a mixing length model [14].

$$U_m = 0.95 \frac{DU_o}{y_c} \sqrt{\frac{\rho_v}{\rho_l}} \tag{1}$$

$$y_c = 0.11(x - L) + 0.3D \tag{2}$$

$$\frac{T_m(x-L)}{T_{pool}} = e^{-y_c}\left[0.36(x-L) + 1.8D\right] \tag{3}$$

$$\frac{T_m(x-L)}{T_{pool}} = e^{-y_c}\left[0.36e^{0.17(x-L)} + 2.5D\right] \tag{4}$$

To predict the maximum velocity (U_m) of the turbulent jet along the axial direction with Eq. (1), we need a priori knowledge of the characteristic length of the jet width (y_c).

The results of applying the correlation predicting y_c (Eq. (2)) into the test data show that the agreement between the predicted values and measured values in the test data has an error rate ±10% (Fig. 2(b)). This is because *x*-*L* is the length from the end of the steam jet penetration length (*L*) [15] to the measured location (*x*) along the axial direction; moreover, it accounts for the variation of the mass flux of the steam jet and the temperature of the tank water. As shown in Fig. 2(c), the maximum velocity (U_m) between the test data and the values predicted by Eq. (1) are also in good agreement (with the error of ±10%) because the y_c term in Eq. (1) governs the accuracy of the predicted value of U_m. However, the maximum temperatures of the turbulent jet (T_m) along the axial direction are not accurately predicted by the correlation in Eq. (3), which was previously developed for a horizontal steam discharging condition at a distance of 8 cm to 16 cm from the exit of the steam discharge nozzle. Thus, we propose the new correlation in Eq. (4) which has an error rate of about ±10% when compared to the test results (Fig. 2(d)). Fig. 2(e) and 2(f) compare the normalized radial velocity and temperature between the test results and Tollmien's theory [8,14] for an expansion coefficient, *a*, of 0.082 (Table 3) at the axial locations of 10 cm, 20 cm, and 30 cm from the exit of the steam discharging nozzle.

Using Tollmien's theory, we found good agreement with the test data for the predicted velocity profiles (U/U_m) along the radial direction with $a = 0.082$ and for the predicted temperature profile ($\Delta T/\Delta T_m$) at 10 cm but not for the normalized radial temperature profiles at the axial locations of 20 cm and 30 cm with $a = 0.082$; the latter values are about 10% to 15% higher than the test data. However, this difference may be neglected because the average pool water temperature (T_{pool}) in the experiment was usually increased by 2ºC to 3ºC during the measuring period in each test run due to the high enthalpy of the steam jet and the rather limited volume of subcooled water pool. This change of average temperature may affect the normalization process of the test data along the radial direction at each axial location, whereas Tollmien's theory assumes a constant value for the pool water temperature. We can therefore conclude that the turbulent jet induced by the steam jet discharged thorough the vertical upward nozzle can be modeled by the empirical correlations and Tollmien's theory with a coefficient of a = 0.082; these were developed on the basis of horizontal steam jet discharge condition. This coefficient value is about 10% to 30% larger than the recommended coefficients for a single phase jet [14]; the increase is due to the effect of entrainment and expansion phenomena developed in the steam jet condensation process. The correlation of the predicted maximum temperature of the turbulent jet along the axial direction was modified on the basis of the new teat data.

3. CFD ANALYSIS

3.1 Modeling Strategy and Grid Model

A previous CFD analysis [7,8] shows that ANSYS CFX-11 [16] can be used with a model of the steam condensation region to predict the velocity and temperature of a turbulent water jet produced by a condensing steam jet discharged into a subcooled water pool. The CFD prediction for the velocity and temperature of the turbulent jet over a distance of 8 cm to 16 cm from the exit of the steam discharge nozzle with a 1 cm diameter is mainly dependent on the turbulent intensity value given at the inlet condition; the inlet is located at the outlet of the region defined by the model of the steam condensation region [8].

Table 3. Similarity Method for Tollmien's Theory [15]

Flow field	Heat transfer
$\frac{U}{U_m} = f\left(\frac{y}{x}\right) = f(\eta)$	$\frac{\Delta T}{\Delta T_m} = \theta\left(\frac{y}{x}\right) = \theta(\eta)$
$U = \frac{m}{x}\frac{F'(\eta)}{\eta}, \quad V = \frac{m}{x}\left[F'(\eta) - \frac{F(\eta)}{\eta}\right]$	$\Delta T = \Delta T_m \theta(\eta) = \frac{k}{x}\theta(\eta)$
$UV + \frac{1}{y}\frac{\partial}{\partial x}\int_{\infty}^{y} U^2 y dy + c^2 x^2\left(\frac{\partial U}{\partial y}\right) = 0$	$\Delta TV + \frac{\partial}{\partial x}\int_{\infty}^{y} \Delta TU dy + c^2 x^2 \frac{\partial U}{\partial y}\frac{\partial T}{\partial y} = 0$
$\left[F''(\varphi) - \frac{1}{\varphi}F'(\varphi)\right]^2 = F(\varphi)F'(\varphi)$	$c^2\theta'(\eta)\left[F''(\eta) - \frac{F'(\eta)}{\eta}\right] = F(\eta)\theta(\eta)$
$\varphi = \frac{y}{ax}, \quad a = \sqrt[3]{c^2}, \quad \frac{U_m}{U_o} = 0.96 \Big/ ax/R_o$	$\frac{\Delta T}{\Delta T_m} = \theta(\eta) = \sqrt{\frac{F'(\eta)}{\eta}} = \sqrt{\frac{U}{U_m}}$

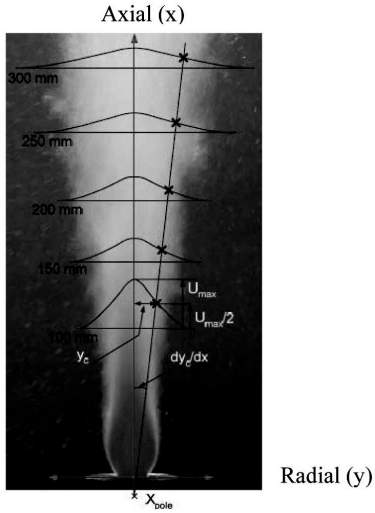

(a) Conceptual description of the steam-driven turbulent jet

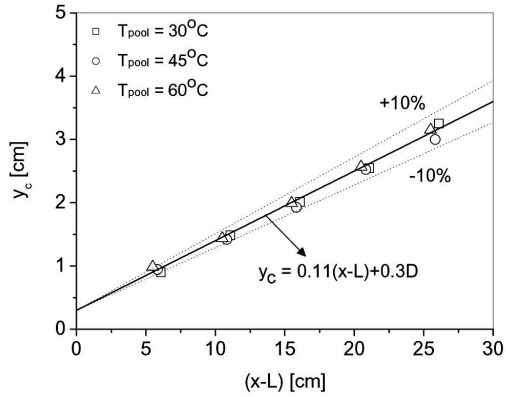

(b) The characteristic length of the jet width

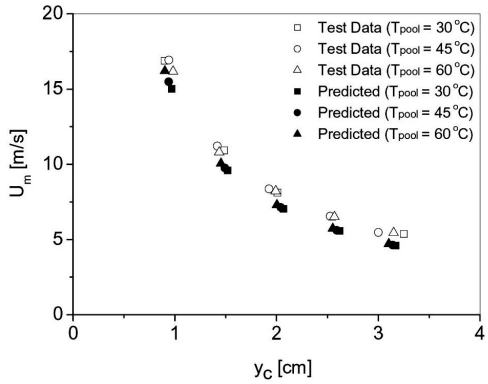

(c) The maximum velocity along the jet centerline

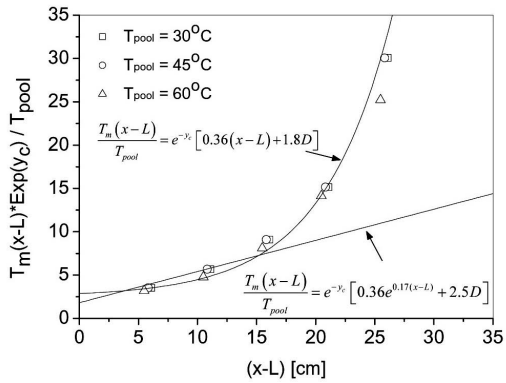

(d) The maximum temperature along the jet centerline

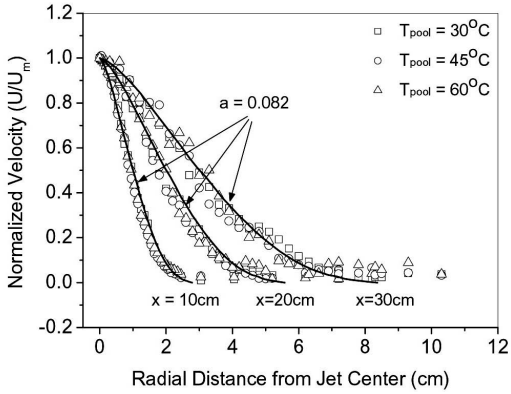

(e) The normalized velocity along the radial direction

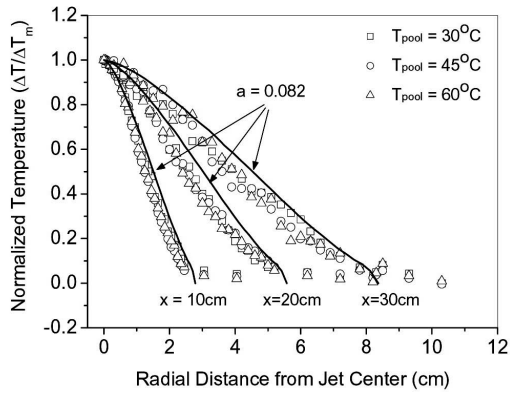

(f) The normalized temperature along the radial direction

Fig. 2. Comparison of the Predicted Values by the Correlations and Tollmien's Theory with the Test Data for a Steam Jet of 900 kg/m^{2}s (Where x is the Distance from the Exit of the Steam Discharge Nozzle and L is the Steam Penetration Length.)

However, the CFD analysis of the test results was not validated in previous works because the measured test data were derived solely from the inner region of the turbulent jet width (y_c) [8,11]. For a complete validation of the CFD method of analysis, we therefore need to undertake a CFD analysis with the recommended flow field and numerical models derived from previous CFD results [8]. The test case for the new CFD analysis includes conditions of a steam mass flux of 900 kg/m^{2}s and a pool temperature of 45ºC. These values differ slightly different from the conditions of the previous research [8]: namely, a steam mass flux of 1000 kg/m^{2}s and a pool temperature of about 30ºC.

An axisymmetric grid model that has a fine hexahedral mesh with a cell length of 1 mm to 10 mm (Fig. 3) is used because the turbulent jet behaviour has an axisymmetric flow pattern from the center of the vertical upward steam discharge hole in the experiment. The axisymmetric calculation also saves computational time. In the grid

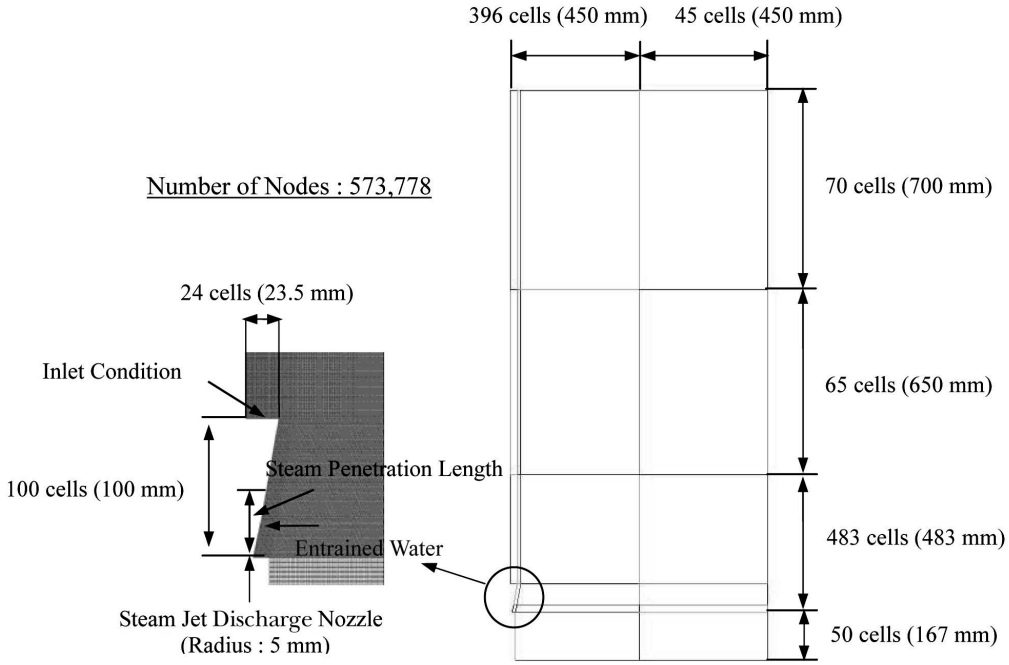

Fig. 3. Axisymmetric Grid model

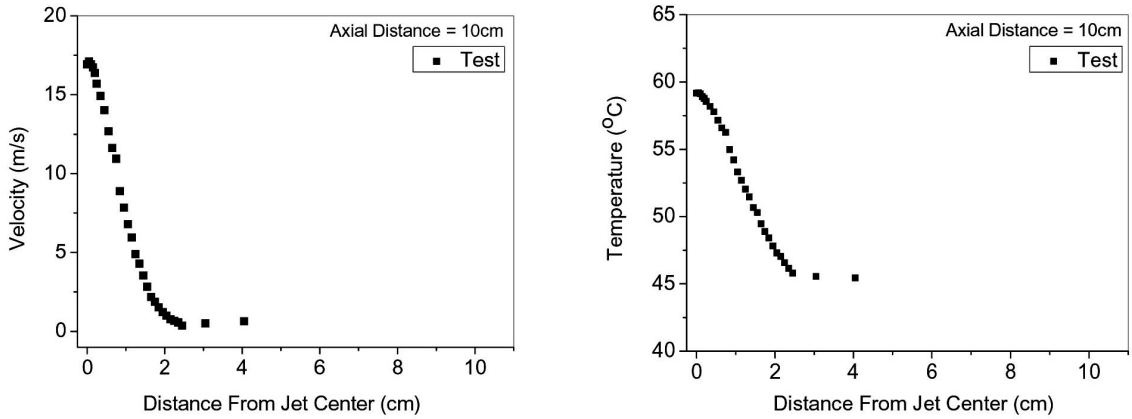

Fig. 4. Inlet Boundary Conditions Values at 10 cm from the Exit of the Steam Discharge Nozzle

model, we exclude the turbulent jet boundary and the flow region from the vertical upward steam discharge hole to an axial location of 10 cm with a radius of about 2 cm in the radial direction inside the steam. These values are excluded so that the CFD calculation can be started from the turbulent jet region at the axial distance of 10 cm. The purpose of this modeling is to evaluate the CFD prediction values against the test data for axial locations in the ranges of 15 cm to 30 cm. We perform this evaluation before applying the CFD calculation to other regions in the subcooled water pool so that we can get a better understanding of the overall thermal mixing behavior in a pool. The CFD analysis of the turbulent jet is performed in a transient state because the local thermal mixing pattern of the pool water is in proportion with the discharge time of the steam jet. However, it is difficult to simulate the entire steam discharge time in the test, and the local velocity and temperature behaviour at x = 10 cm to 30 cm may be less dependent on the steam discharge time. Accordingly, we performed a transient calculation of 10 s calculation with a time step of 0.0001 s.

3.2 Boundary Conditions and Governing Equations

The inlet boundary condition, the Dirichlet condition [16], was set at an axial location of 10 cm with a length of 4 cm in the radial direction (Fig. 3). Fig. 4 shows the velocity and temperature distributions of the test data at an axial location of 10 cm. The value of the turbulent intensities at the inlet was set as 40% of the mean velocity because the eddy motions are very actively generated when the steam jet is discharged into the subcooled water through the steam discharge nozzle. The entrainment model of the subcooled water [7] was introduced to simulate the subcooled water flowing into the steam jet at the boundary region of the steam penetration length. The pressure outlet boundary condition, the Neumann condition [16], was set for the upper region of the pool, which only allows an outflow of air.

On the basis of previous CFD results [8], the behavior of the turbulent jet induced by the steam jet in the subcooled water pool was treated as an incompressible flow, a free air surface over the pool water, a turbulent flow, and a buoyancy flow. Therefore, the governing equations (Eqs. (5) to (8)) used in this study are the Navier-Stokes equation and the energy equations with a homogenous multifluid model under a coupled algorithm [16]. The turbulent flow is simulated by the shear stress transport model (Eqs. (9) to (11)) and the buoyancy is modeled by the full density model [16]. A high resolution model is used for the numerical model of the convection term [16]. In the homogenous model, the interphase mass and heat transfer is neglected. Each transport quantity in the governing equations except for the volume fraction is summed over all the phases to provide a single transport quantity. As a calculation method, 10 to 20 iterations were performed with a time step of 0.0001 s until the mass, enthalpy, and velocity residual of the water reached a value of less than 1.0E-04.

$$\frac{\partial}{\partial t}\left(\gamma_\alpha \rho_\alpha\right)+\nabla\bullet\left(\gamma_\alpha \rho_\alpha V_\alpha\right)=0 \tag{5}$$

$$\frac{\partial}{\partial t}\left(\gamma_\alpha \rho_\alpha V_\alpha\right)+\nabla\bullet\left[\gamma_\alpha\left(\rho_\alpha V_\alpha\otimes V_\alpha-\mu_\alpha\left(\nabla V_\alpha+\left(\nabla V_\alpha\right)^T\right)\right)\right]=\gamma_\alpha\left(B-\nabla P_\alpha\right) \tag{6}$$

$$\frac{\partial}{\partial t}\left(\gamma_\alpha \rho_\alpha h_\alpha\right)+\nabla\bullet\left[\gamma_\alpha\left(\rho_\alpha V_\alpha h_\alpha-\lambda_\alpha\nabla T_\alpha\right)\right]=0 \tag{7}$$

$$\rho=\sum_{\alpha=1}^{N_p}\gamma_\alpha\rho_\alpha,\quad V=\frac{1}{\rho}\sum_{\alpha=1}^{N_p}\gamma_\alpha\rho_\alpha V_\alpha \tag{8}$$

$$\frac{\partial(\rho k)}{\partial t}+\nabla\bullet\left(\rho V k\right)=\nabla\bullet\left[\left(\mu+\frac{\mu_t}{\sigma_{K1}}\right)\nabla k\right]+P_k-\beta'\rho k\omega \tag{9}$$

$$\begin{aligned}&\frac{\partial(\rho\omega)}{\partial t}+\nabla\bullet\left(\rho V\omega\right)=\nabla\bullet\left[\left(\mu+\frac{\mu_t}{\sigma_{\omega3}}\right)\nabla\omega\right]\\&+\left(1-F_1\right)2\rho\frac{1}{\sigma_{\omega3}\omega}\nabla k\nabla\omega+\alpha_3\frac{\omega}{k}P_k-\beta_3\rho\omega^2\end{aligned} \tag{10}$$

$$\nu_t=\frac{a_1 k}{\max\left(a_1\omega, SF_2\right)} \tag{11}$$

3.3 Discussion on the CFD Results

To compare the CFD results of the transient state with the test results of the quasi-steady state, we need to check the time dependency of the CFD results. The velocity, temperature, and normalized velocity distributions along the radial and axial directions at 8 s, 9 s, and 10 s are shown in Figs. 5 to 6. The local phenomena at the region between the inlet and the free surface show no dependency on the simulation time except for the temperature distribution at the outer region of the turbulent jet width (that is, A in Fig. 6(e) and B in Fig. 6(e)). As shown in Fig. 5, the turbulent jet discharged from the inlet propagates up to the free surface and changes direction towards the tank wall before finally moving downward due to a strong entrainment flow that develops around the steam jet. This circulation flow mixes the turbulent jet with the subcooled water well, and then the local temperature at the outer region of the

turbulent jet width is continually increased as shown in A in Fig. 6(e) and B in Fig. 6(e). However, this temperature increase may be neglected because the positions of the temperature extracted in the CFD computation domain are located around the boundary of the turbulent jet. The important data to be compared with the test data are located inside the boundary of the turbulent jet. Furthermore, the test data at the same locations increase with time due to the strong circulation flow, which is driven by the steam jet discharge. A comparison of the normalized velocity profiles along the radial direction at the different axial locations of x = 15 cm and 25 cm shows that the time dependency can be neglected. We therefore selected the CFD results at 10 s for comparison with the test results.

A comparison of the normalized velocity and temperature profiles along the radial direction at the axial locations of 15 cm, 20 cm, 25 cm, and 30 cm are shown in Figs. 7 to 8. These figures also plot the prediction results of Tollmien's theory with a = 0.082. The comparison shows that the CFD results accurately predict the local phenomenon of a turbulent jet downstream of a steam jet with an error rate of 10% except for the temperature at the outer regions of the

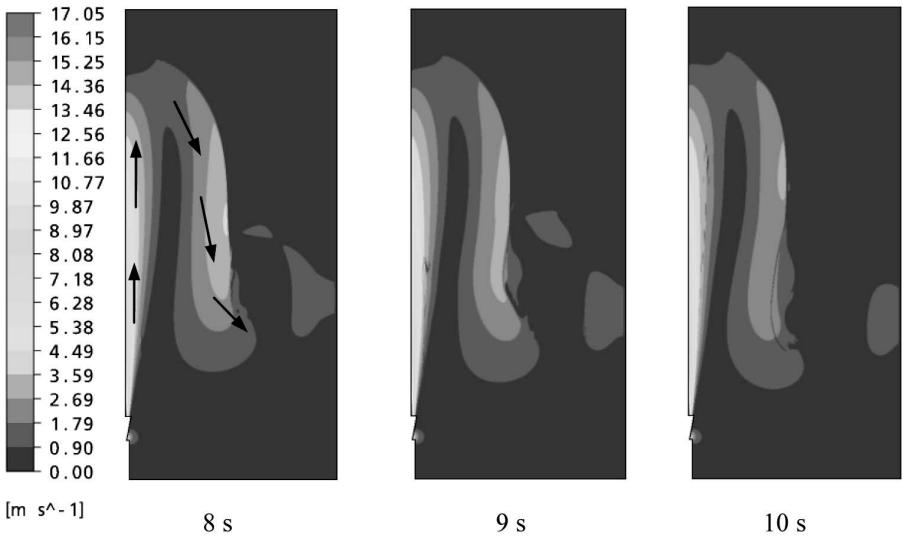

(a) Velocity distribution contours

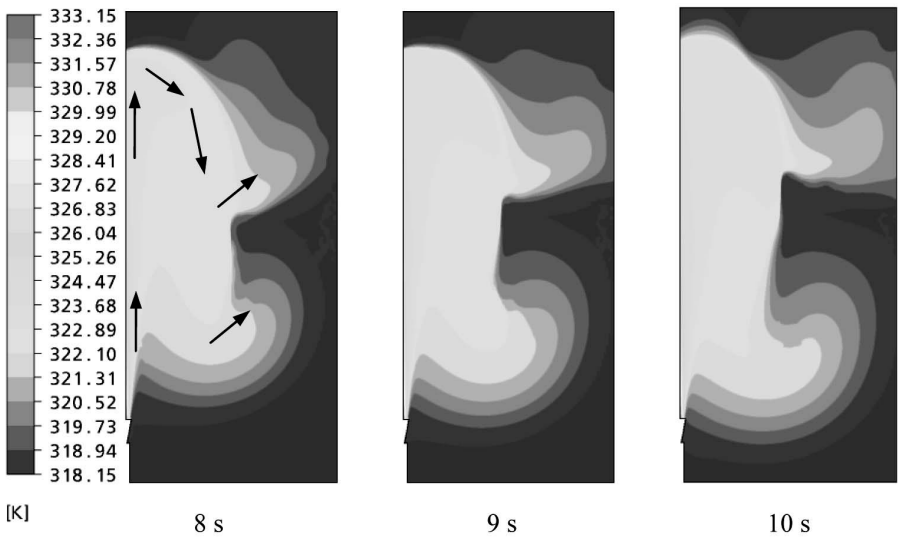

(b) Temperature distribution contours

Fig. 5. Velocity and Temperature Distribution of the CFD Results (Steam Mass Flux = 900 kg/m^{2}s; Pool Temperature = 45ºC)

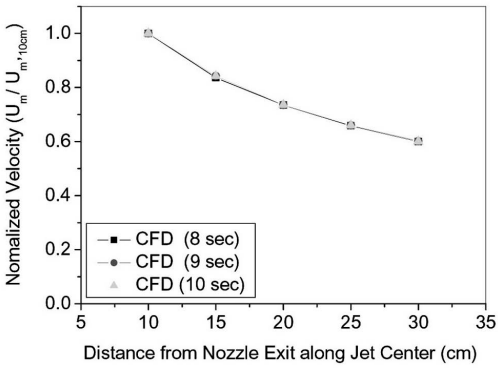

(a) Normalized velocity along the jet centerline

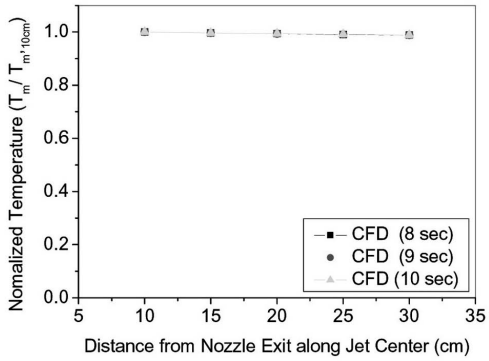

(b) Normalized temperature along the jet centerline

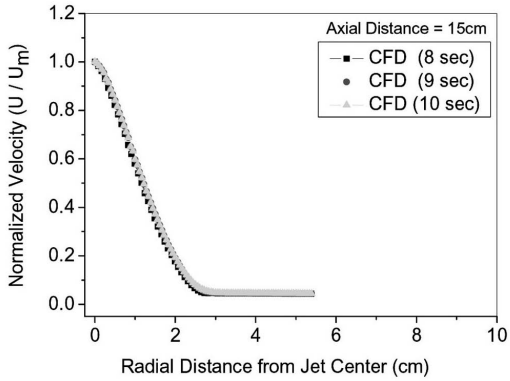

(c) Normalized velocity along the radial direction at 15 cm

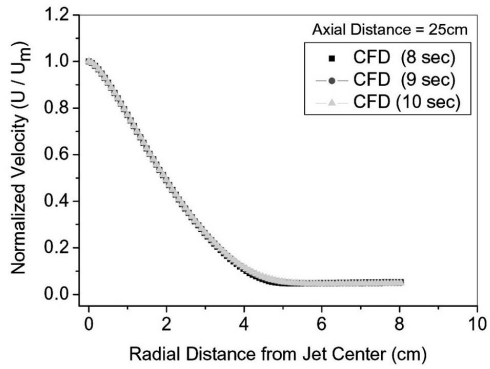

(d) Normalized velocity along the radial direction at 25 cm

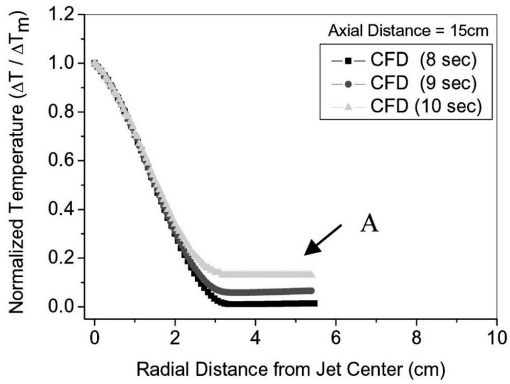

(e) Normalized temperature along the radial direction at 15 cm

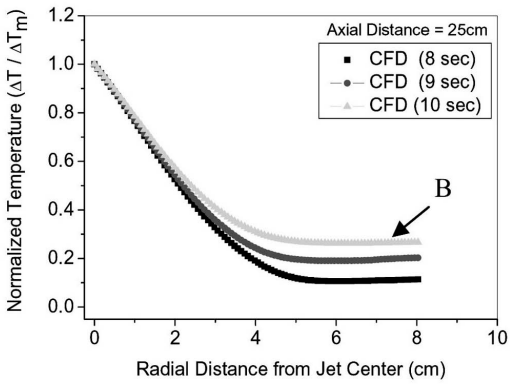

(f) Normalized temperature along the radial direction at 25 cm

Fig. 6. Normalized Velocity and Temperature at the Jet Centerline and Axial Locations of 15 cm and 25 cm (Steam Mass Flux = 900 kg/m^{2}s; Pool Temperature = 45ºC)

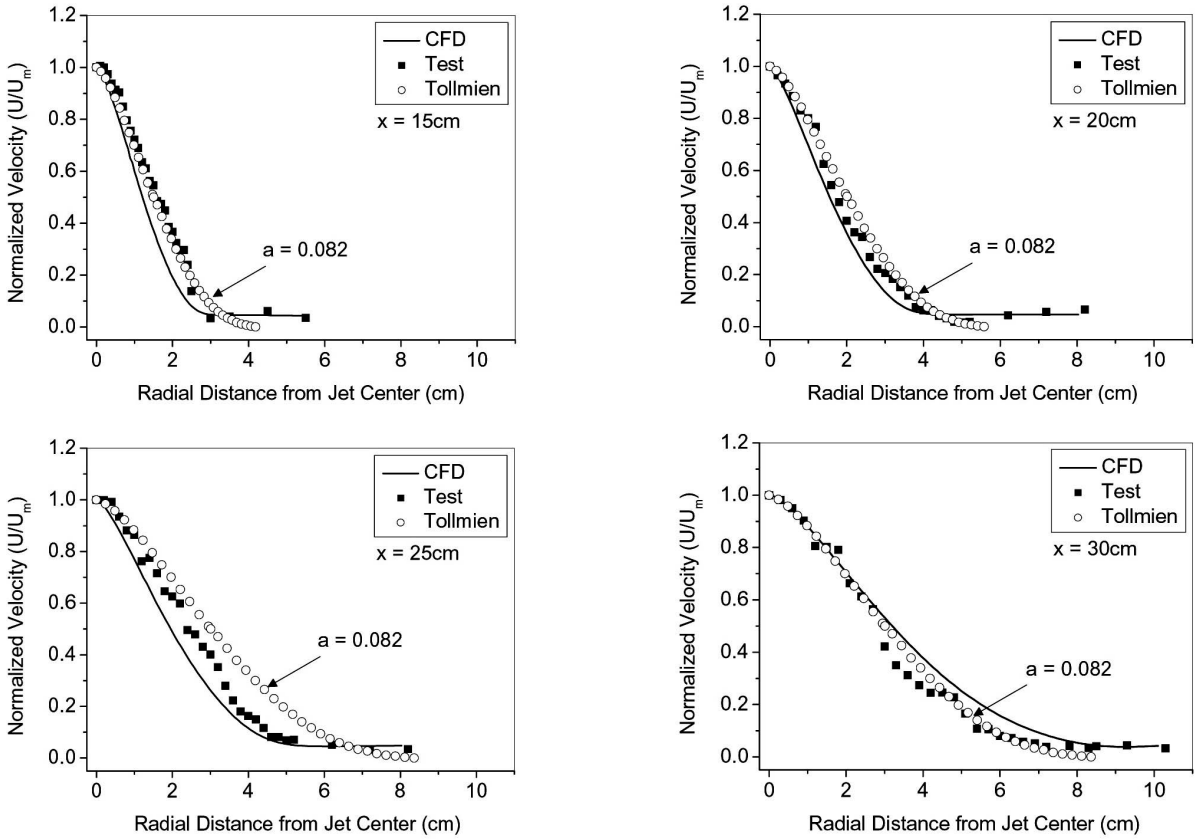

Fig. 7. Comparison of the Normalized Velocity Along the Radial Direction at the Axial Locations of 15 cm, 20 cm, 25 cm, and 30 cm (Steam Mass Flux = 900 kg/m^{2}s; Pool Temperature = 45ºC)

turbulent jet width (that is, the A, B, C, and D regions of Fig. 8). Thus, as shown in Fig. 7, the results confirm that the 40% turbulent intensity value given at the inlet region of the turbulent jet plays an important role in enlarging the boundary of the turbulent jet width through the momentum diffusion process along the radial direction. According to a comparison of the temperature (Fig. 8) in the CFD results and the test results, the CFD results also accurately predict the test data because the turbulent temperature field is calculated from the velocity results by using the turbulent Prandtl number of 0.9 [16,17]. However, a further discussion of the temperature difference between the CFD results and the test data is not helpful because the temperature values of the outer regions of the turbulent jet width (the A, B, C, and D regions of Fig. 8) in the experiment were not measured at the same time. The movable pitot tube and TC spool were moved from the outer region of the turbulent jet width to the jet center, and the velocity and temperature at each location were measured for a 5 s period. Thus, the temperature measured at the outer region of the turbulent jet width in the experiment was reported as the value of the initial pool temperature. The CFD results extracted for comparison with the test data were all measured at 10 s. In addition, the average pool temperature was increased in a short time due to the strong circulation flow induced by the turbulent jet. This time difference produced the temperature difference shown in the A, B, C, and D regions of Fig. 8. In general, we can conclude that the CFD analysis offers a reasonable simulation of the local phenomenon of a turbulent jet downstream of a steam jet but only when the CFD analysis reflects the physics of a high intensity of the turbulent jet induced by condensing jets.

4. CONCLUSION

The velocity and temperature of a turbulent jet in a subcooled water pool are very important because the behavior of the turbulent jet give directly affects the local temperature of the subcooled water that is entrained into a steam jet; and this behavior consequently affects the overall pattern of thermal mixing in a pool. If the local temperature of the entrained water increases above a certain limit, unstable condensation may occur and damage the

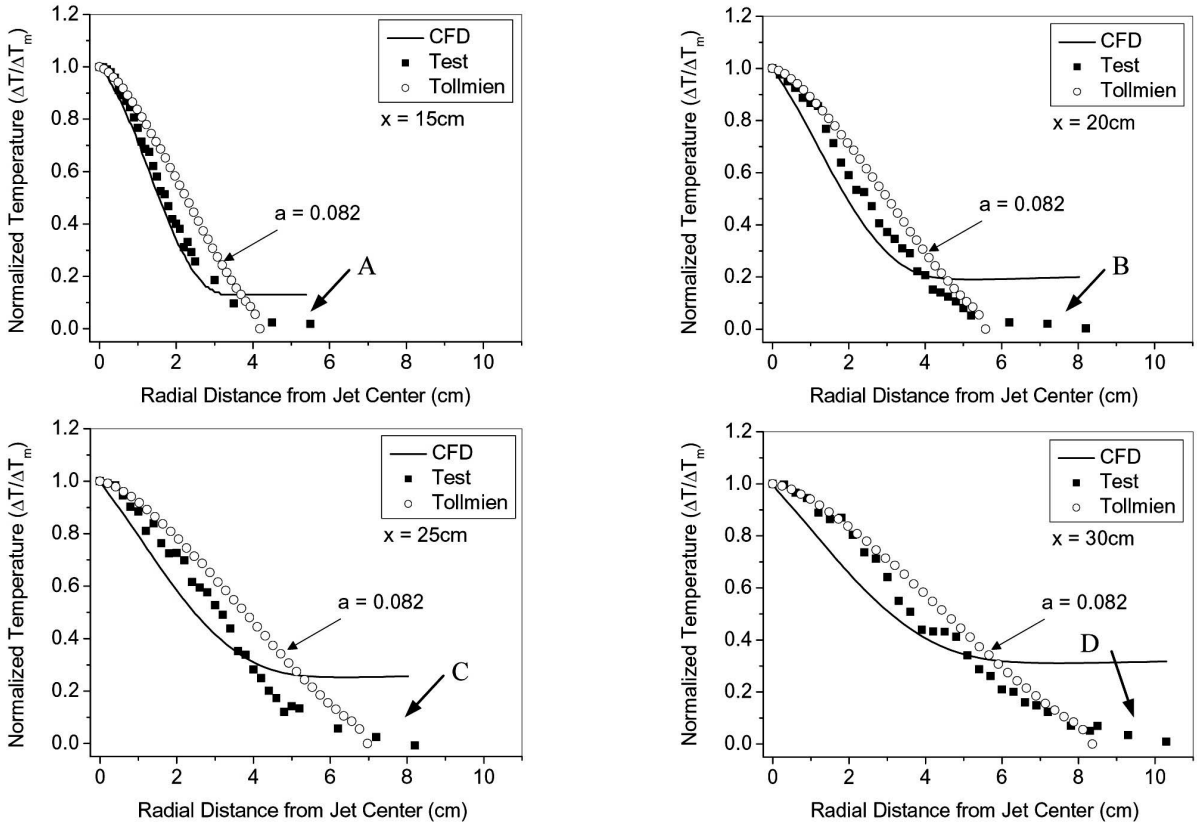

Fig. 8. Comparison of Normalized Temperature Along the Radial Direction at the Axial Locations of 15 cm, 20 cm, 25 cm and 30 cm (Steam Mass Flux = 900 kg/m^{2}s; Pool Temperature = 45ºC)

integrity of the internal structures and the wall of the pool.

The CFD method of analysis previously developed to predict the velocity and temperature profiles of a turbulent jet was validated with the new small-scale test data performed under a vertical steam discharge condition, which can accurately simulate an axisymmetric flow pattern in a subcooled water pool. To extend the applicability of this method, we compared its performance with that of a turbulent jet model developed on the basis of empirical correlations and Tollmien's theory with $a = 0.082$.

With the recommended model of the high turbulent intensity of 40% for the turbulent jet and a fine mesh grid model with a cell length of 1 mm to 10 mm, the CFD analysis accurately predicted the test results well with an error rate of 10%. We can therefore conclude that the turbulent intensity value of the turbulent jet is the most important factor because it enlarges the boundary of the turbulent jet through which the momentum and heat transfer diffusion process actively occur along the radial direction. This phenomenon strongly affects the length of the jet boundary along the axial direction. A comparison of the CFD results and test results of the turbulent jet behavior confirm that this enlarged momentum diffusion process is related to the fact that the expansion coefficient of a = 0.082 in Tollmien's theory is larger than that of a single-phase jet. The results confirm that the empirical correlations used to predict the maximum velocity (U_m) and the characteristic length of the jet width (y_c) can be applied to the new test data with an error rate of 10%. Here, the correlation used to predict the maximum temperature (T_m) along the jet centerline was modified on the basis of the new test data.

As a further work, new large-scale experiments with CFD analysis are needed to validate the new method, particularly with regard to characterization of the overall circulation phenomena induced by condensing steam jets in a pool. Ultimately, a new approach to the CFD analysis of condensing jet-induced thermal mixing in a pool should be developed for direct analysis of the steam jet condensation phenomena. The new approach should ideally obviate the need for simple models, such as a steam condensation region model which are usually derived from sophisticated experiments.

NOMENCLATURE

a expansion coefficient in jet theory
D diameter of the vertical upward single hole [cm]
y_c radial characteristic length from the centerline to the location of $0.5U_m$ [cm]
k turbulent kinetic energy [m^2/s^2]
T_{pool} temperature of the subcooled water pool [ºC]
ΔT temperature difference of the steam and jet at an arbitrary location (= T (x,y) - T_{pool}) [ºC]
ΔT_m temperature difference of the steam and jet at the centerline (= T_m - T_{pool}) [ºC]
U_m maximum velocity at the jet centerline [m/s]
U_o steam velocity at the exit of the steam nozzle [m/s]
x distance from the single-hole center in a horizontal direction [cm]
y distance from the single-hole center in a vertical direction [cm]

Greek symbols

ε eddy dissipation [m^2/s^3]
ν molecular viscosity [m^2/s]
ν_t turbulent viscosity [m^2/s]
ρ density [kg/m^3]
ω eddy dissipation frequency [1/s]
λ thermal conductivity [W/mK]
γ volume fraction

ACKNOWLEDGEMENTS

This work was supported by the Nuclear Research & Development Program of the National Research Foundation (NRF), through a grant funded by the Ministry of Education, Science and Technology (MEST) of the Korean government. (Grant code: M20702040003-08M0204-00310).

REFERENCES

[1] C.-H. SONG and H.-C. KIM, "OECD/NEA Experts' Activities on the Application of CFD Codes to Nuclear Reactor Safety Problems: Issues and Future Direction", Trans. the Korean Nuclear Society Autumn Meeting, Gyeongju, Korea, October 29-30 (2009)
[2] Mahaffy, J. (ed.) "Best Practice Guidelines for the Use of CFD in Nuclear Reactor Safety Applications", OECD, Nuclear Energy Agency, Technical Report, CSNI/R(2007)5, April (2007)
[3] Smith, B.L. (ed.), "Assessment of Computational Fluid Dynamics (CFD) for Nuclear Reactor Safety Problems", OECD Nuclear Energy Agency, Technical Report, NEA/CSNI/R(2007)13, Jan. (2008)
[4] D. Bestion, H. Anglart, J. Mahaffy, D. Lucas, C.H. Song, M. Scheuerer, G. Zigh, M. Andreani, F. Kasahara, M. Heitsch, E. Komen, F. Moretti, T. Morii, P. Mühlbauer, B.L. Smith, T. Watanabe, Extension of CFD Codes to Two-Phase Flow Safety Problems, NEA-CSNI-R(2010)2, (2010)
[5] C.-H. Song, W.-P. Baek & J.-K. Park, "Thermal-Hydraulic Tests and Analyses for the APR1400 Development and Licensing", *Nucl. Eng. & Technol*., Vol. 39, pp. 299-312 (2007)
[6] C.-H. Song et al., "Development of the PIRT for Thermal Mixing Phenomena in the APR1400 IRWST", *Proc. 5th Korea-Japan Symposium on Nuclear Thermal-Hydraulics and Safety* (NTHAS5), Jeju, Korea, Nov. 26-29 (2006)
[7] H.S. Kang and C.-H. Song, "CFD Analysis for Thermal Mixing in a Subcooled Water Tank under a High Steam Mass Flux Discharge Condition," *Nucl. Eng. Des*. **238**(3), pp. 492-501 (2008).
[8] H.S. Kang and C.-H. Song, "CFD Analysis of a Turbulent Jet Behavior Induced by a Steam Jet Discharge through a Single Hole in a Subcooled Water Tank," *Nucl. Eng. Des*. **240**(9), pp. 2160-2168 (2010).
[9] R.J.E. Van Wissen, K.R.A.M. Schreel and C. W. M. V. Van Der Geld, "Particle Image Velocimetry Measurement of a Steam-Driven Cofined Turbulent Water Jet," J. *Fluid Mech.* **530**, pp. 358-368 (2005).
[10] T.M. Su, "Suppression pool temperature limits for BWR containments," United States Nuclear Regulatory Commission, NUREG-0783 (1981).
[11] Y.S. Kim and Y.J. Yoon, "Experimental Study of Turbulent Jet Induced by Steam Jet Condensation through a Hole in a Water Tank," *Int. Com. in heat and Mass Transfer*, **35**, pp. 21-29 (2008).
[12] Y.-J. Youn, Y.-J. Choo, Y.-S. Kim, and C.-H. Song, "Velocity and Temperature Profiles of a Turbulent Jet Induced vy a Steam Jet Discharge into a Subcooled Water Pool," Proc. of 7th International Topical Meeting on Nuclear Reactor Thermal Hydraulics, Operation and Safety (NUTHOS-7), Seoul, Korea, Oct. 5-9, (2008).
[13] C.-H. Song et al., "Characterization of Direct Contact Condensation of Steam Jets Discharging into a Subcooled Water, " *IAEA Technical Committee Meeting*, PSI, Villigen (1998).
[14] G.N. Abramovich, The Theory of Turbulent Jets, MIT Press, Boston, pp. 76-85 (1963).
[15] H.Y. Kim, A Study on the Characteristics of Direct Contact Condensation of a Steam Jet Discharging into a Quenching Tank through a Single Horizontal Pipe, Ph.D Thesis, KAIST (2001).
[16] ANSYS Inc., CFX-11 Manual, (2008).
[17] Adrian Bejan, Convection Heat Transfer, 2nd, John Wiley & Sons, Inc., (1995).